

WEAR OF ABRADABLE COATINGS
Towards multi-physics analyses for the design of turbomachines

Mathias Legrand¹
Post-Doctoral Fellow

Christophe Pierre
Dean of the Faculty of Engineering
Structural Dynamics and Vibration
Laboratory
Department of Mechanical
Engineering
McGill University
Montréal, Québec, Canada

ABSTRACT

Better turbomachine performances are achieved by reducing possible parasitic leakage flows through the closure of the clearance distance between blade tips and surrounding casings. Accordingly, direct contact is now considered as part of aircraft engines normal life.

In order to avoid possibly catastrophic scenarios, implementation of abrasible coatings has been widely recognized as a robust solution. Nevertheless, the process of wear undergone by abrasible coatings is not well understood. In the present work, its macroscopic behavior is numerically approximated through a piecewise linear plastic constitutive law which allows for real time access to the abrasible layer profile.

First results prove convergence in time and space of the proposed approach and show that the frequency content of the blade response is clearly affected by the presence of abrasible coatings. It seems that the opening of the clearance between the blade tip and the casing due to wear leads to large amplitudes of motion far from the usual linear conditions.

INTRODUCTION

Facing a constant need of improved performances for lower operating costs, jet engine manufacturers respond with the reduction of possible parasitic leakage flows by closing the gap between blade tips and surrounding casings. This is made possible through the implementation of abrasible coatings [1] in the compressor and turbine sections where a minimal clearance is required.

The mechanical properties of the abrasible material are of primary importance as it must preserve the incurring blade-tips from damage by being reasonably soft, but also be sufficiently hard to stand very high temperatures and high-speed gas flows with inherent solid particles. It has been detected during test runs that erosive wear of abrasible coatings may play a significant role in the rise of divergent behaviors such as propagating cracks in blade roots. Accordingly, it seems urgent to enrich the limited current knowledge of the circumstances under which they occur [2].

Modeling the erosion process in a macroscopic manner seems rather new [3] even though simple analytical derivations do exist [4]. This task is difficult because of the complex and coupled physical mechanisms involved such as dislocation, thermal gradients, large displacements and mass removal [5]. In turbomachines, where large relative displacements between contacting components together with high abrasible wear rates are observed, most of the existing theoretical statements do not seem relevant and easy to implement [6].

It is here assumed that plasticity with its inherent abilities to represent permanent deformation in a simple fashion stands as a natural first macroscopic approach in order to account for abrasible coatings erosive wear. It is thought that the behavior of the blade will be properly predicted.

¹Corresponding author. Email: mathias.legrand@mcgill.ca

1 STRUCTURAL MODEL AND EQUATIONS OF MOTION

The present study deals with a single rotating blade and a surrounding casing of a low pressure compressor stage, as depicted in Fig. 1(a). Within the well-known finite element framework under the assumption of small displacements, vector \mathbf{u} stores all the displacement degrees-of-freedom of the blade and the respective mass matrix \mathbf{M} , damping matrix \mathbf{D} , stiffness matrix \mathbf{K} and contact forces \mathbf{F}^c are built accordingly. The resulting governing equations of motion take the form:

$$\mathbf{M}\ddot{\mathbf{u}} + \mathbf{D}\dot{\mathbf{u}} + \mathbf{K}\mathbf{u} + \mathbf{F}^c = \mathbf{0} \quad (1)$$

complemented with the usual contact constraints.

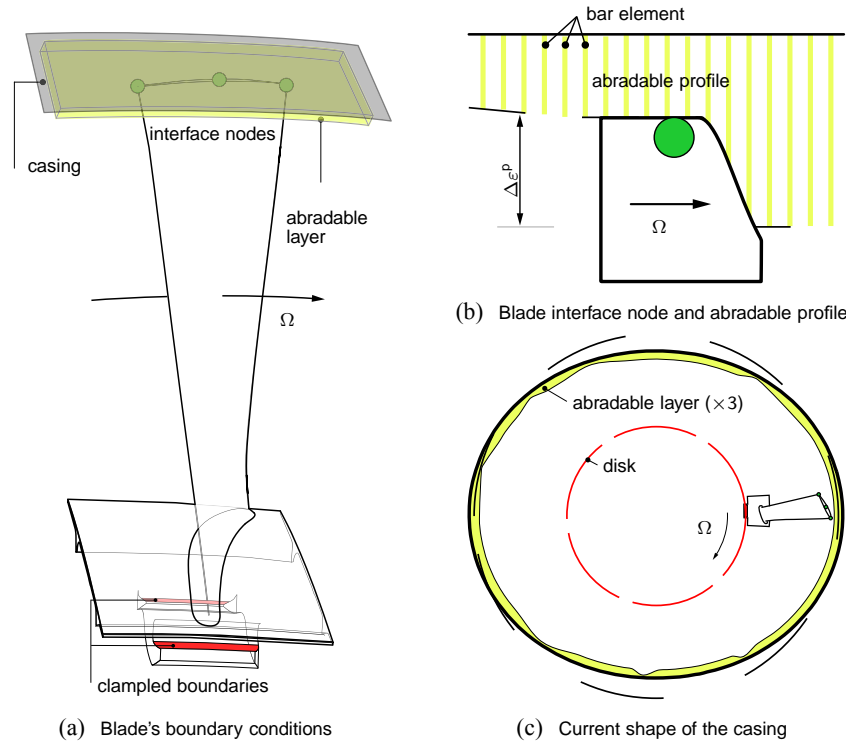


Figure 1 – Blade under investigation

The introduced finite element model of the blade is numerically too large and leads to cumbersome computation times. It is reduced through the Craig-Bampton procedure [7] where three interface nodes (leading edge, middle of the chord and trailing edge) define the contact interface with the casing, so that the contact constraints can directly be treated in the reduced space (see Fig. 1(a)). Since the chosen Craig-Bampton interface nodes of the blade, as such, do not contain any information about the *true* geometry of the blade tip, this has to be numerically included in the solution method, as illustrated in Fig. 1(b), in order to ensure space convergence of the abrasible profile.

Moreover, thorough preliminary simulations showed that the casing is insensitive to the contact interaction with the blade and is not modeled as a flexible component.

2 ABRADABLE CONSTITUTIVE LAW WITH PLASTICITY

As a first approach, the abrasible coating is discretized with the usual one-dimensional two-node bar elements, as displayed in Fig. 1(b), undergoing a nonlinear plastic constitutive law. By convention, strains ε and stresses σ are such that $(\varepsilon, \sigma) \in \mathbb{R}^+ \times \mathbb{R}^+$. The set of admissible stresses \mathbb{E}_σ is defined as follows [8]:

$$\mathbb{E}_\sigma = \{(\sigma, \alpha) \in (\mathbb{R}, \mathbb{R}) \setminus f(\sigma, \alpha) \leq 0\} \quad (2)$$

where $\alpha : [0, T] \rightarrow \mathbb{R}$ is an internal hardening variable and f , a yield function. It is also assumed that (1) the total strain is separated in an additive way between its elastic part ε^e and plastic part ε^p such

as $\varepsilon = \varepsilon^e + \varepsilon^p$ and (2) the relation between elastic strains and stresses is linear $\sigma = E\varepsilon^e$. By choice hardening is isotropic. This leads to:

$$f(\sigma, \alpha) = \sigma - (\sigma_Y + K\alpha) \quad (3)$$

where $\sigma_Y > 0$ stands for the elastic limit and $K \geq 0$, for the plastic modulus of the abradable material. The second assumption yields:

$$\Delta\alpha = \Delta\varepsilon^p \quad (4)$$

and condition on the plastic flow implies the existence of a consistency parameter γ , such as $\Delta\varepsilon^p = \gamma \frac{\partial f}{\partial \sigma}$, equivalent to $\Delta\varepsilon^p = \gamma$ because of Eq. (3). Dual variables γ and f obey the Kuhn-Tucker conditions, complemented by the consistency condition:

$$\gamma \geq 0; \quad f(\sigma, \alpha) \leq 0; \quad \gamma f(\sigma, \alpha) = 0; \quad \gamma \Delta f(\sigma, \alpha) = 0 \quad (5)$$

For a one-dimensional quasi-static strain formulation, the solution strategy is greatly simplified. Consider an admissible state together with an imposed increment of deformation $\Delta\varepsilon$ within a purely elastic trial state:

$$\sigma^{\text{trial}} = E\Delta\varepsilon + \sigma; \quad \Delta\varepsilon^p = 0; \quad \Delta\alpha = 0; \quad f^{\text{trial}} = \sigma^{\text{trial}} - (\sigma_Y + K\alpha) \quad (6)$$

In order to ensure that the trial state belongs to \mathbb{E}_σ , f^{trial} has to be tested:

- if $f^{\text{trial}} \leq 0$, trial and current states coincide;
- if $f^{\text{trial}} > 0$, condition (5)₂ is violated and the trial state has to be corrected. The commonly adopted approach, named *Return Mapping Algorithm* [9], relies on the projection of the trial state on the boundary of the yield function $f = 0$ together with condition $\gamma > 0$ at constant strain. Variation of Eq. (3) yields:

$$f = f^{\text{trial}} - \gamma(E + K) \quad (7)$$

Consequently, $f = 0$ implies:

$$\gamma = \frac{f^{\text{trial}}}{E + K} \quad (8)$$

and the following update is used:

$$\sigma = \sigma^{\text{trial}} - E\gamma \quad \text{and} \quad \Delta\alpha = \Delta\varepsilon^p = \gamma \quad (9)$$

During a contact phase, the virtual work of the internal forces acting within the abradable coating for a virtual displacement $\delta\mathbf{u}$ of the blade is equal by definition to the virtual work of the contact force for the same virtual displacement. By defining $I = \{i \mid g(i) = 0\}$ (blue bar elements in Fig. 1(b)), equilibrium of the contact forces with the internal forces can be written as:

$$\mathbf{F}^c = \sum_{i \in I} A_i \sigma_i \quad (10)$$

where A_i stands for the cross-section area of an abradable element and depends on the density parameter.

3 TIME MARCHING PROCEDURE

The phenomenon under investigation is inherently transient and making use of time stepping techniques seems fairly natural. For non-smooth and non-differentiable nonlinear terms such as those mentioned above, explicit algorithms seem more relevant [10] and are adopted here.

By noting \mathbf{u}_{n+1} , the numerical approximation of the exact value $\mathbf{u}(t_{n+1})$ at time $t_{n+1} = t_n + h$ where h is the time-step, the classical explicit central finite difference scheme used in this work yields:

$$\ddot{\mathbf{u}}_n = \frac{\mathbf{u}_{n+1} - 2\mathbf{u}_n + \mathbf{u}_{n-1}}{h^2} \quad \text{and} \quad \dot{\mathbf{u}}_n = \frac{\mathbf{u}_{n+1} - \mathbf{u}_{n-1}}{2h} \quad (11)$$

The contact detection as well as the internal force contribution of the abradable material are handled by employing the prediction/correction technique developed in [11]. The final algorithm is then divided into four steps:

1. **prediction**, at time step $n + 1$, of the displacements \mathbf{u} of the blade by neglecting the abradable coating. This predicted displacement, denoted with subscript p , is expressed as:

$$\mathbf{u}_{n+1,p} = \left[\frac{\mathbf{M}}{h^2} + \frac{\mathbf{D}}{2h} \right]^{-1} \left(\left(\frac{2\mathbf{M}}{h^2} - \mathbf{K} \right) \mathbf{u}_n + \left(\frac{\mathbf{D}}{2h} - \frac{\mathbf{M}}{h^2} \right) \mathbf{u}_{n-1} \right) \quad (12)$$

where displacements \mathbf{u}_n and \mathbf{u}_{n-1} are known.

2. **determination** of the gap function $\mathbf{g}_{n+1,p}$ between the two contacting components. A search algorithm identifies all abradable elements $i \in I$ being penetrated by the blade contact interface.
3. **abradable internal forces computation** through a deformation increment $\Delta\varepsilon$ induced by the predicted penetrations between the two bodies. Subsequent strains $\sigma_{i \in I}$, hardening variables $\alpha_{i \in I}$ and plastic deformations $\varepsilon_{i \in I}^p$ are updated using the above mentioned procedure. The final vector of internal forces is calculated through Eq. (10) and the abradable profile is updated.
4. **displacement correction** consistent with the calculated contact forces [11, 12]:

$$\mathbf{u}_{n+1} = \mathbf{u}_{n+1,p} - \left[\frac{\mathbf{M}}{h^2} + \frac{\mathbf{D}}{2h} \right]^{-1} \mathbf{F}^c \quad (13)$$

4 RESULTS

4.1 Configuration of interest

It is here assumed that a temperature gradient equivalent to a multi-harmonic two-nodal diameter load quasi-statically distorts the casing in order to absorb the initial clearances, as depicted in Fig. 1(c). The wear level is governed by the plastic law parameters E , K and σ_Y illustrated in Fig. 2 and two configurations, respectively with low and high wear, are later investigated. The convergence in space

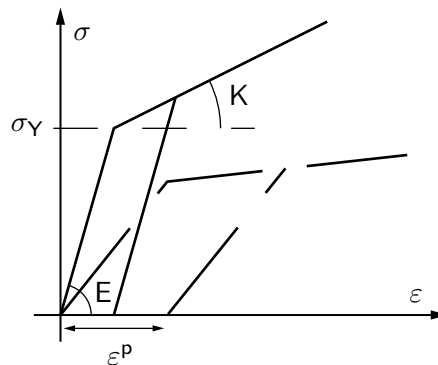


Figure 2 – Definition of the plasticity constitutive law for low (—) and high (—) wear

and time of the erosion wear law is checked. This is respectively achieved by increasing the density of abradable elements and by reducing the time-step of the numerical tool but is not displayed here for the sake of brevity.

4.2 Modal analysis and wear profile

Within the operating range of a low pressure compressor, only the first flexural mode is expected to be excited in a dangerous manner through direct contact. Its frequency is denoted by f_1 with respect to which are normalized all the frequency results and rotational velocities Ω .

A series of simulations has been conducted in order to understand the sensitivity of the abradable wear law and subsequent profile to the rotational velocity Ω . Beforehand, a quick modal analysis of the blade as a linear flexible structure is required to better understand the up-coming results. Since the casing keeps a multi-harmonic two-nodal diameter shape during interaction, the first frequency of the blade will be reached for Ω such as:

$$\Omega \text{ (Hz)} = \frac{f_1}{k} \text{ (Hz)}, \quad k = 2, 4, 6 \dots \quad (14)$$

that describes engine-order lines crossing the first frequency of resonance of the blade. In Eq. (14), k is limited to even positive integers due to the assumed shape of the casing. This condition will thus be satisfied for lower rotational velocities. In what follows, we pay attention to $k = 4$ and $k = 6$ since $k = 2$ is out of the operating range in terms of Ω .

It is well known that direct unilateral contact conditions stiffen the interacting mechanical components and modify their frequency of resonance. Accordingly, Eq. (14) could be revisited as follows:

$$\Omega \text{ (Hz)} = \frac{f_1(|\mathbf{F}^c|)}{k} \text{ (Hz)}, \quad k = 2, 4, 6 \dots \quad (15)$$

where $|\mathbf{F}^c|$ simply refers to the amplitude of the contact forces.

Amplitude maps in Figs. 3(a) and 3(b) explicitly show the wear level in the abradable coating along the circumferential direction of the casing with respect to Ω and implicitly indicate the number of worn lobes. For low or high rotational velocities, the shape of the casing controls the wear profile since the blade does not respond in resonance to the nonlinear contact excitation and only two lobes are worn. On the contrary, when Eq. (15) is satisfied, large amplitudes of vibration are expected: this is clearly shown for $k = 4$ and $k = 6$ where four lobes and six lobes are distinguishable, respectively. The contact stiffening effect is well caught by the proposed algorithm since, in Figs. 3(a) and 3(b), the worn lobe highest amplitudes should be located at $\Omega = 0.25$ ($k = 4$) and 0.16 ($k = 6$) based on Eq. (14) but are located at $\Omega = 0.31$ ($k = 4$) and $\Omega = 0.21$ ($k = 6$) instead, see Eq. (15).

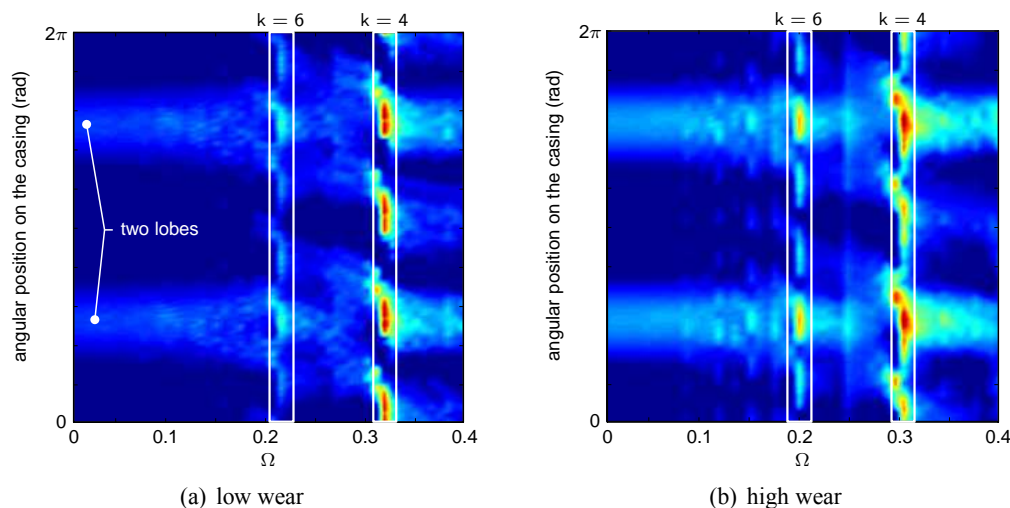


Figure 3 – Map of the final abradable profiles with respect to Ω for interface node 1 after ten rounds of the blade

In other words, the first flexural mode of the blade is excited through intermittent contact with the casing increasing the level of erosion wear for very specific Ω . Nevertheless, the abradable ductility, determined by mechanical parameters E , K and σ_Y do modify the conditions of interaction. As can be seen in Figs. 3(a) and 3(b) again, the rotational velocities for which the blade is in resonance are slightly different, depending on the level of wear.

Obviously, all the presented results strongly depend on the adopted scenario of interaction and further investigations have to be conducted to better understand the mechanisms of wear and possible divergence. Nevertheless, they seem in good agreement with experimental observations about possible and unexpected severe vibration problems.

CONCLUSION

The emphasis of the study has been placed on the understanding of the contact interaction occurring between a blade and a surrounding casing belonging to the low pressure compressor of an aircraft engine. The study focuses on modeling, in a realistic and macroscopic fashion, the erosion wear law of abradable coatings which are used to soften the direct contact between interacting components.

First results show that the developed model provides understandable and consistent physical results. It seems that by opening the operating clearance between the blade tip and the casing, larger motions may be expected far from the usual interaction conditions provided by the well-known Campbell diagrams.

In order to better estimate the wear parameter, comparisons with experimental results such as the ones presented in [13, 14] have to be scheduled in a near future.

References

- [1] Yi, M., He, J., Huang, B., and Zhou, H., 1999. "Friction and wear behaviour and abrasability of abradable seal coating". *Wear*, **231**(1), pp. 47 – 53.
- [2] Jiang, J., Ahrens, J., Ulbrich, H., and Scheideler, E., 1998. "Contact model of a rotating rubbing blade". In Proceedings of the 5th International Conference on Rotor Dynamics of the IFTOMM, pp. 478 – 489.
- [3] Salles, L., Blanc, L., Thouverez, F., and Gousskov, A., 2008. "Analysis of a bladed disk with friction and fretting-wear in blade attachments". In Proceedings of GT2008 ASME Turbo Expo 2008: Power for Land, Sea and Air, no. GT2008-51112.
- [4] Rabinowicz, E., 1965. *Friction and wear of materials*. John Wiley & Sons, Inc., New-York.
- [5] Andrews, K. T., Shillor, M., Wright, S., and Klarbring, A., 1997. "A dynamic thermoviscoelastic contact problem with friction and wear". *International Journal of Engineering Science*, **35**(14), pp. 1291 – 1309.
- [6] Strömberg, N., Johansson, L., and Klarbring, A., 1996. "Derivation and analysis of a generalized standard model for contact, friction and wear". *International Journal of Solids and Structures*, **33**(13), pp. 1817 – 1836.
- [7] Craig, R., and Bampton, C., 1968. "Coupling of substructures for dynamics analyses". *AIAA Journal*, **6**(7), pp. 1313 – 1319.
- [8] Simo, J., and Hughes, T., 1998. *Computational inelasticity*. Springer.
- [9] Simo, J., and Taylor, R., 1986. "A return mapping algorithm for plane stress elastoplasticity". *International Journal for Numerical Methods in Engineering*, **22**, pp. 649 – 670.
- [10] Vola, D., Pratt, E., Raous, M., and Jean, M., 1998. "Consistent time discretization for a dynamical contact problem and complementarity techniques". *Revue Européenne des Éléments Finis*, **7**, pp. 149 – 162.
- [11] Carpenter, N., Taylor, R., and Katona, M., 1991. "Lagrange constraints for transient finite element surface contact". *International Journal for Numerical Methods in Engineering*, **32**, pp. 130 – 128.
- [12] Legrand, M., Pierre, C., Cartraud, P., and Lombard, J.-P., 2009. "Two-dimensional modeling of an aircraft engine structural bladed disk-casing modal interaction". *Journal of Sound and Vibration*, **319**(1-2), pp. 366 – 391.
- [13] Padova, C., Dunn, M., and Barton, J., 2008. "Casing treatment and blade tip configuration effects on controlled gas turbine blade tip/shroud rubs at engine conditions". In Proceedings of GT2008 ASME Turbo Expo 2008: Power for Land, Sea and Air, no. GT2008-50112.
- [14] Peyraut, F., Seichepine, J.-L., Coddet, C., and Hertter, M., 2008. "Finite element modeling of abradable materials - identification of plastic parameters and issues on minimum hardness against coating's thickness". *International Journal for Simulation and Multidisciplinary Design and Optimization*, **2**, pp. 209 – 215.